CAVITATION WEAR ON CENTRIFUGAL PUMP IMPELLENTS MADE FROM HASTELLOY C-276 ALLOY

Tomás Fernánde-Columbié*; Jorge Luis Reyes-de la Cruz.; Isnel Rodríguez-González.; Ledennis Suárez-Torres.

Universidad de Moa "Dr. Antonio Núñez Jiménez". Ave. Calixto García #15, entre Ave. 7 de Diciembre y calle Reynaldo Laffita, Las Coloradas, Moa. Holguín. Mechanical Department. www.ismm.edu.cu

tfernández@ismm.edu.cu, jreyes@ismm.edu.cu, irgonzalez@ismm.edu.cu, lstorres@ismm.edu.cu

ABSTRACT

This article establishes the incidence of the leached liquor in the wear, by cavitation, of impellers of a centrifugal pump. The impeller blades, manufactured from the Hastelloy C-276 superalloy, were analyzed. Eight samples which were sectioned from the upper end of the blade, less affected, to the tip of the blade, more damaged. Through scanning electron microscopy (SEM), pitting, rupture of the passive layer, crumbling of the structure, as well as intercrystalline corrosion were evidenced on the surface. It was observed, in diffractograms, the presence of chlorine (Cl), chemical element that forms chloride ions, which prevents the formation of stable layers of oxides. As a result of this phenomenon, the hardness increased from 225 HV to 270 HV, after the analyzed impellers were removed from service.

Keywords: *cavitation, blades, wear, leached liquor, Hastelloy C-276*

INTRODUCCIÓN

Among the difficulties encountered in the transport of the fluid in the mining industry are the effects on the resistance of the materials used in the manufacture of impellers for centrifugal pumps, so that it can cope with the phenomenon of cavitation. The nickel-based superalloy Hastelloy C-276 has been frequently used to guarantee the durability of operation in these turbomachines, however, due to the particularities of the leached liquor, a multi-component mixture, liquid composed of gases, vapors and solids, which damages the entire system, making transfer difficult, due to the implosion effect of the bubbles on the impellers and the volute (Reyes-Cruz *et al.*, 2019).

Material wear is a problem in different industries and in most cases, it is mainly due to the abrasion and erosion caused by the sand present in the fluid. Several mechanisms of erosive wear and semi-empirical equations have been proposed to model the rate of wear, these equations contain in their expression two constants characteristics of the material: its fracture toughness and its hardness (Meng and Ludema, 1995; Durán-Martínez and Fernández-Columbié, 2018).

Of the studies carried out on cavitation in centrifugal pumps, those of Friedrichs and Kosyna (2002); Reyes (2007) stand out, which show that the pressure and flow rate fluctuations are created by the blades as they pass through the spiral chamber tab during the occurrence of the cavitation phenomenon. In addition to the instabilities created by opening or closing valves during the operation of pumps, difficulties related to transmission lines appear.

Shi et al. (2013); Xiao *et al*. (2016) explain that the fluctuations in pressure and flow are caused by an oscillation of the dynamics of cavitation, within the cavitation and, that this occurs when the flow varies abruptly. The mentioned above fluctuations produce a flow that causes the formation of bubbles separated from the liquid and which collapse together, providing instability to the fluid. They conclude that the phenomenon of cavitation involves the formation and presence of bubbles, a product of the change of phase of the substance from its liquid state to the state of vapor.

Reyes (2007) and Reyes (2010) propose that, there are agents that intervene in the presence of cavitation phenomenon and generalize it in different fundamental factors related to the fluid: temperature, vapor pressure, fluid density, physical-mechanical properties, gas concentrations, chemical composition, solid phase concentrations and pH.

Mechanism of wear caused by cavitation

In the study of the cavitation phenomenon, several materials and thermal, thermomechanical and thermochemical treatments have been used in the search for the improvement of the resistance to this type of wear. On the side of the alloys, the most varied families have also been tested, such as iron castings, nickel and cobalt based alloys, stainless steels, nonferrous alloys (Guo et al., 2016).

According to Alcantara *et al.* (2016), wear, together with corrosion and fatigue, are the three main processes that limit or degrade the life of engineering products, which causes the loss of performance of the part or mechanical systems. The C-276 Hastelloy super alloy has been designed to resist these phenomena under both oxidizing and reducing conditions. It is used to manufacture mechanical elements used in the mining industry.

Stechmann *et al.* (2015) and Reyes (2015), state that as a consequence of the formation, growth and implosion of bubbles, erosion and detachment of impeller blade material can occur on the surface. The size of the bubbles varies constantly, oscillates in time before their disappearance and the pressure suffers rapid variations.

DEVELOPMENT

The chemical composition of the Hastelloy C-276 super alloy is shown in table 1. It was determined in a quantum mass spectrometer, according to the standards established for this purpose.

Table 1. Hastelloy C-276 alloy chemical composition, % by mass

Mo	Cr	Fe	W	Co	Mn	C	V	Ni
15,0	16,0	4,0	3,8	2,5	0,9	0,01	0,35	57,44

In the nickel-based super alloys the secondary phase forming chemicals Cr, Mo, W, Nb. The added carbon in the range of 0.05 - 0.2 %, combines with reactive and refractory elements such as titanium, tantalum and hafnium, to form carbides such as $M_{23}C_6$ and M_6C, which tend to accumulate at the grain boundary during heat treatment or operation at high temperatures.

Metallographic preparation of the samples

The cutting operation was carried out in a vertical milling machine, taking into account that the samples used were excessively large, as shown in figure 1, it was necessary to reduce them to a size that allowed its handling (15 x 15 x 32 mm), (ASTM E 92 Standard). This cut was made in such a way that an analysis could be made in all the areas affected by the fluid and then, from these areas, the mechanical metallurgical variations that arise in them could be established. After polishing, the samples were chemically attacked with 10 % mixture of nitric and hydrochloric acids.

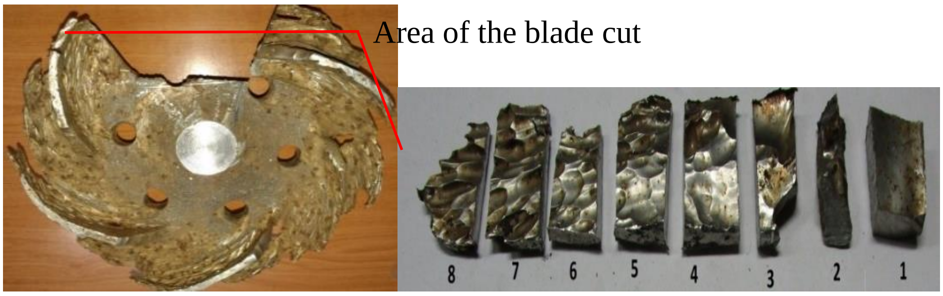

Figure 1. Cut made to a blade of selected samples.

In order to determine the standard microstructure of the blades (Hastelloy C-276), a binocular optical microscope brand NOVEL model NIM-100 was used, equipped with a camera that allows obtaining photos of the microstructure. Figure 2 (samples under conditions of 27 and 34 % of leached liquor) shows a matrix structure with the ferrite in the grain edge and austenite, which is of the dendritic type, which is indicative of a previous treatment to obtain it. These characteristic phases are developed during the smelting process, because the dendrite appears as a result of temperature gradients and originates in the direction of such gradient.

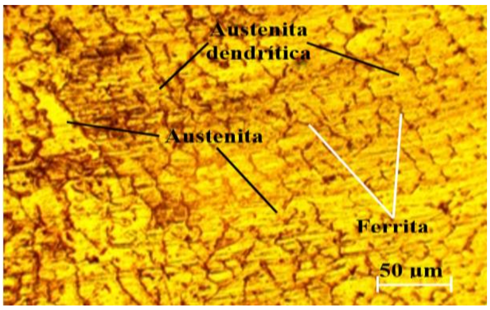

Figure 2. Pump blades structure.

Scanning Electron Microscopy was performed under vacuum (LV-5600). The anode acceleration voltage was 20 kV, with secondary electron imaging (SEI) modes in "High-Vac" type up to 3.5 nm and by backscattered electrons.

To determine the hardness, 4 blades were finned, as shown in figure 3. These areas were considered, taking into account the incidence of the fluid on them. Of the 8 samples cut, No. 1; 4; 6, were 8 also selected for hardness scanning. These were chosen because, when the bubbles implode, the effect on the blades is not homogeneous.

Figure 3. Hardness measurement in the different selected areas

Discussion and analysis of results

Microstructural analysis of impeller blade cavities

When the cavities is analyzing in the pump blades, it can be seen that, for a liquor concentration of 27 % (figures 4(a) and (b)), the cavitation phenomenon starts with small holes and cracks on the surface, leaving it susceptible due to the effect of the components present in the fluid. While, for a concentration of 34 % (Figures 5(a) and (b)), this defect increases with greater intensity, in the matrix the holes and cracks occur all along the grain boundaries. As the liquor concentrate increases, so do the cavities in the impeller blades, leading to deterioration of the crystalline structure of the alloy.

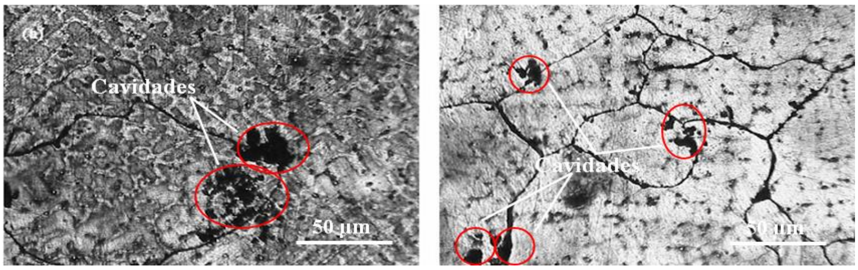

Figure 4(a) and (b). Blade surface cavities for 27 % concentration.

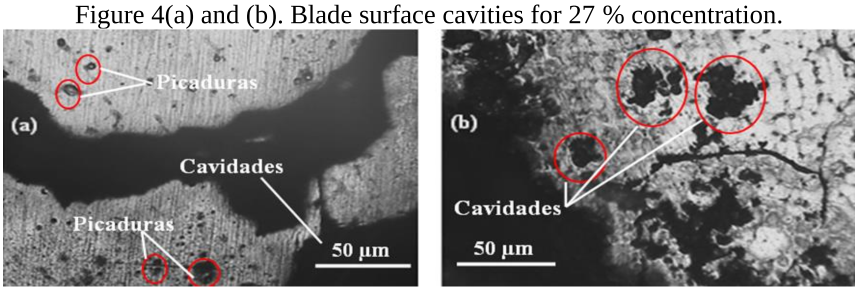

Figure 5(a) and (b). Blade surface cavities for 34% concentrations.

The onset of cavitation is due to points of fluid breakage on the surface of the alloy called cavities. These points are the tension necessary to break or fracture the liquid, i.e. overcome the intermolecular cohesion forces and start the formation of flaws or discontinuities on the surface of the alloy.

Evaluation of the damage on the passive layer

The behavior obtained, by means of SEM, figures 6(a) and (b), correspond to a 27% concentration on the surface of the Hastelloy C-276 super alloy, which shows a lower incidence of cavitation. Regardless of this condition, there is a damaged structure with the formation of pitting and the breaking of the passive layer, with the presence of carbides. The fluid has caused a widespread attack by the effect of intercrystalline corrosion, with the presence of cracks along the grain boundary. There is a line of grains that show crumbling, which weakens the passive layer and the mechanical resistance of the material.

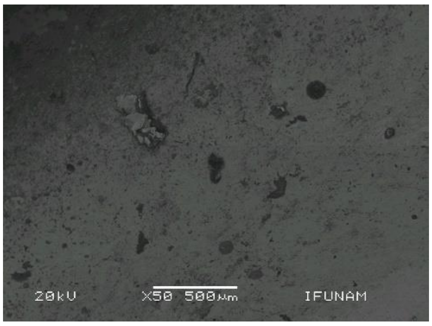

Figure 6(a). Sample 1.

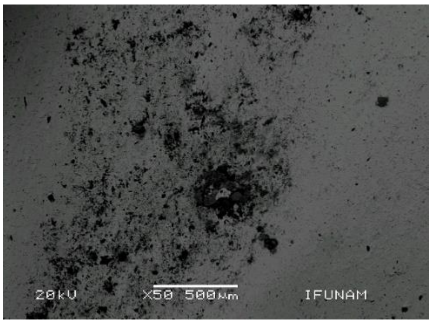

Figure 6(b). Sample 2.

Figure 6(c). Sample 1.

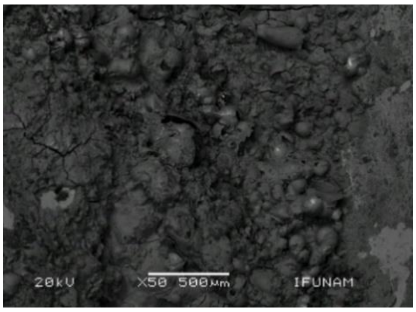

Figure 6(d). Sample 2.

For 34 % concentration in the fluid (figures 6(c) and (d)), the material shows a more deteriorated surface with the presence of pores, cracks and carbides, there is a deformation of the dendritic phase and a non-textured matrix. The formation of the dark shade present on the surface, can be associated with the incrustations of the liquor in the grain boundaries, which leaves it susceptible to superalloy, giving rise to the phenomenon of cavitation.

As there is a greater implosion of the bubbles, more deformation is introduced in the surface of the material, the tensional state is uniaxial with homogeneous distribution of the tensions, the plastic flow is confined in this zone, remaining in a state of plastic load, where radial and circumferential tensions appear, which give rise to a state of compound tensional on the material, criterion that has been reported by authors like Barzdaitis et al.

The SEM standards obtained in the different samples (Figure 7(a)), correspond to 27% of concentration and 7(b) to 34 %. An angle of 45.51º was used to obtain the diffractograms. It is observed that, there is a variation in the chemical elements, as the fluid interacts with the surface of the Hastelloy C-276 superalloy, the components of this hydro mixture leave the material susceptible to the phenomenon of cavitation, the bubbles influence the durability of the impeller. The presence of oxidizing or reducing substances, traces of CO2 and organic substances in the solution can change this character and make the steels active or passive. There is a surface hardening as a result of the successive impacts of the shock waves that produce the appearance and implosion of the vapor bubbles generated by the cavitation process, which favors localized transformation with low levels of effort (Mittag and Gabi, 2015).

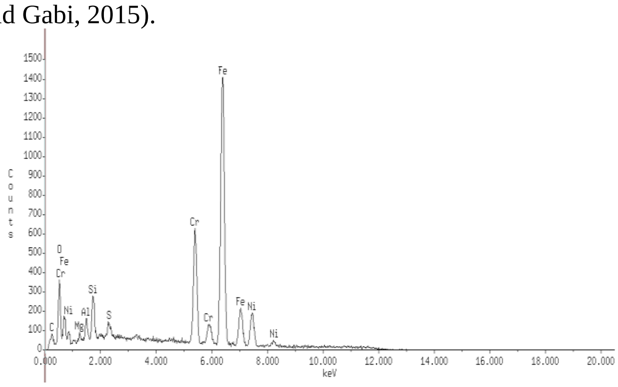

ZAF Correction Acc.Volt.= 20 kV Take-off Angle=45.51 deg
Number of Iterations = 5

Element	k-ratio (calc.)	ZAF	Atom %	Element Wt %	Wt % Err. (1-Sigma)	No. of Cations
C -K	0.0120	3.946	15.28	4.73	+/- 0.37	18.447
O -K	0.0437	1.873	19.87	8.19	+/- 0.35	---
Al-K	0.0068	2.185	2.13	1.48	+/- 0.10	2.576
Si-K	0.0151	1.696	3.53	2.55	+/- 0.09	4.262
Cr-K	0.1616	0.914	11.03	14.77	+/- 0.28	13.320
Fe-K	0.5404	1.043	39.18	56.37	+/- 0.64	47.314
Ni-K	0.0941	1.095	6.81	10.30	+/- 0.52	8.227
Mg-K	0.0021	2.836	0.94	0.59	+/- 0.07	1.138
S -K	0.0079	1.278	1.22	1.01	+/- 0.09	1.477
Total			100.00	100.00		96.761

The number of cation results are based upon 24 Oxygen atoms

Figure 7(a). SEM for 27 % solids concentration in the fluid.

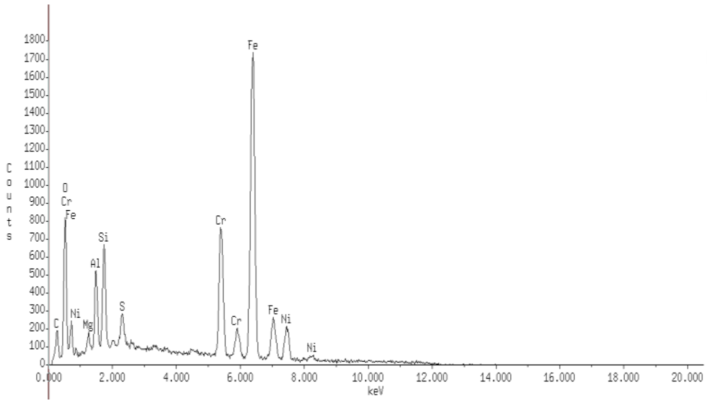

ZAF Correction Acc.Volt.= 20 kV Take-off Angle=45.51 deg
Number of Iterations = 6

Element	k-ratio (calc.)	ZAF	Atom %	Element Wt %	Wt % Err. (1-Sigma)	No. of Cations
C -K	0.0214	4.366	23.99	9.32	+/- 0.35	20.892
O -K	0.0663	2.151	27.56	14.27	+/- 0.36	---
Al-K	0.0170	2.075	4.05	3.53	+/- 0.10	3.525
Si-K	0.0251	1.661	4.58	4.16	+/- 0.09	3.991
Cr-K	0.1313	0.950	7.41	12.47	+/- 0.21	6.456
Fe-K	0.4319	1.069	25.55	46.16	+/- 0.48	22.247
Ni-K	0.0646	1.110	3.78	7.17	+/- 0.38	3.288
Mg-K	0.0035	2.655	1.19	0.93	+/- 0.06	1.034
S -K	0.0119	1.287	1.48	1.53	+/- 0.08	1.285
P -K	0.0014	1.512	0.22	0.22	+/- 0.04	0.188
Cl-K	0.0018	1.238	0.19	0.22	+/- 0.04	0.168
Total			100.00	100.00		63.075

The number of cation results are based upon 24 Oxygen atoms

Figure 7(b). SEM for 34 % solids concentration in the fluid.

The diffractograms show the predominant elements in the Hastelloy C-276 super alloy, nickel, iron, chromium are elements that characterize it, which increase the hardening capacity of the alloy. The mechanical properties of this material, such as its hardness, toughness and elastic limit, make it exhibit characteristics with resistance to abrasive wear and plastic deformation.

Microhardness in the different zones of the blades

When evaluating the hardness behavior in relation to the thickness in one of the worn-out blades removed from service (figure 8), it can be seen that, for an initial value of 217 HV, in the Hastelloy C-276 superalloy, it increased to 225 HV at the upper end of said blade, a matter that is little affected by the effect of the implosion of the bubbles, however, as it approaches the lower end, this property increases until it reaches HV 270.

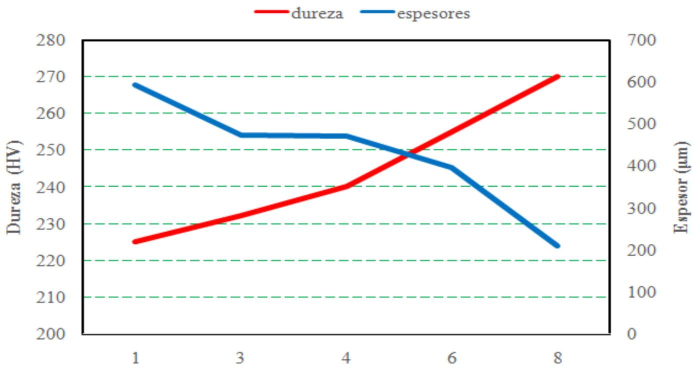

Figure 8. Hardness vs. thickness behavior.

There is an inverse relationship between hardness and thickness, the latter being reduced by the effect of fluid friction on the surface and causing a decrease in grain size due to the effect of pungency.

It could be determined that, during the cavitation phenomenon, which affects the impeller, there is a slide in the grains of the crystalline net, which are produced by the cutting efforts that are manifested in the direction of the flowing crystalline planes, while its magnitude is higher than the characteristic resistance of the crystal. Behaviors that have as a final consequence the formation of dislocation cells by annihilation or recombination and reduction of the energy of the system, giving rise to a structure of sub-grains, within the original grain, therefore, a decrease in the effective size of the crystalline coherence zone.

CONCLUSIONS

1. The incidence of the leached liquor on the surface of the blade, manufactured from the Hastelloy C-276 superalloy, causes the formation of pitting, the breakage of the passive layer, crumbling of the structure, as well as intercrystalline corrosion, a defect promoted by the phenomenon of cavitation.
2. At a concentration of leached liquor of 27%, cavitation begins with small holes and cracks on the surface of the blades, while at 34%, the defects are distributed over the matrix and along the grain boundaries, leaving the surface susceptible to the Hastelloy C-276 superalloy.
3. The hardness increases to 225 HV at the upper end of the blade, an effect that is little affected by the implosion of the bubbles, however, as it approaches the lower end, values of up to 270 HV are obtained.

REFERENCES

Alcántara, D., Fernández, T. y Rodríguez, I. (2016). Influence of leached pulp on wear of a Hastelloy C-276. *Minería y Geología*, *32* (1), 93-105.

Barzdaitis, V., Mažeika, P., Vasylius, M., Kartašovas, V. y Tadžijevas, A. (2016). Investigation of pressure pulsations in centrifugal pump system. *Journal of Vibroengineering, 50* (7), 650-658.

Durán-Martínez, W. y Fernández-Columbié, T. (2018). Effect of corrosion wear on a superalloy exposed to a high concentration of elements in the fluid. *Ciencia & Futuro, 8* (3), 20-31.

Friedrichs, J. y Kosyna. G. (2002). Rotating cavitation in a centrifugal pump impeller of low specific speed. *Journal of Fluids Engineering, 124* (6), 356-362.

Guo, X., Zhu, Z., Cui, B. y Shi, G. (2016). Effects of the number of inducer blades on the anti-cavitations characteristics and external performance of a centrifugal pump. *Journal of Mechanical. Science and Technology, 3* (17), 67-75.

Meng, H. y Ludema K. (1995). Wear models and predictive equations: their form and content. *Wear. 181* (183), 443-457.

Mittag, S. y Gabi, M. (2015). Experimental and numerical investigation of centrifugal pumps with asymmetric in flow conditions. *Journal of Thermal Science, 12* (4): 34-41.

Reyes, J. (2007). Diagnosis of hydro-mixture transport facilities affected by cavitation. *Minería y Geología, 23* (3), 87-117.

Reyes, J. (2010). A teaching and research experiment of cavitation in centrifugal pumps. American Association of Teachers of Physics. *Lat. Am. J. Phys. Educ, 4* (I), 2-18.

Reyes, J. (2015). Saturation pressure of ammonia liquor and its relation to cavitation in centrifugal pumps. *Minería y Geología, 31* (1), 23-30.

Reyes-Cruz, J., Fernández-Columbié, T., Rodríguez-González, I., Ruíz-Chavarría, G. y Hernández-Zapata, S. (2019). Effect of bubble implosion on cavitation wear of centrifugal pumps transferring ammonia fluids. *Minería y Geología, 35* (3), 327-337.

Shi, W., Li, T., Zhang, D. (2013). Effect of tip clearance on the cavitations and flow field of axial flow pumps. *Journal of Huazhong University of Science and Technology: Natural Science Edition, 41* (4): 21-25.

Stechmann, D.; Sese, C., Duvvur, R.; Zhang, A. y Pourpoint, T. (2015). Design and analysis of a high-pressure turbopump at purdue university 51st AIAA/SAE/ASEE. Joint *Propulsion Conference, 24* (13), 76-84.

Xiao, L., Li, Y., Liu, Y., Bi, Z. y Zhao, W. (2016). Effect of wearing clearance on cavitation flow and performance of centrifugal pump with inducer. *Journal of Drainage and Irrigation Machinery Engineering*, 3 (2), 57- 65.